



Optical identification of quantum dot types in CdSe/ZnSe structures

M. Straßburg^{a,*}, Th. Deniozou^a, A. Hoffmann^a, S. Rodt^a, V. Türck^a, R. Heitz^a,
U.W. Pohl^a, D. Bimberg^a, D. Litvinov^b, A. Rosenauer^b, D. Gerthsen^b,
S. Schwedhelm^c, I. Kudryashov^{c,1}, K. Lischka^c, D. Schikora^c

^a*Institut für Festkörperphysik, Technische Universität Berlin, Hardenbergstr. 36, 10623 Berlin, Germany*

^b*Laboratorium für Elektronenmikroskopie der Universität Karlsruhe, Kaiserstr. 12, 76128 Karlsruhe, Germany*

^c*Fachbereich 6 Physik, Universität Paderborn, Warburger Str. 100, 33098 Paderborn, Germany*

Abstract

Two different types of quantum islands, formed either by strain-modified island growth or in the Stranski-Krastanow (SK) mode, were identified by optical and structural investigations. Pronounced differences in the size, shape and Cd content of these islands lead to different localisation energies of three-dimensionally confined excitons allowing a clear distinction of both island types. The classification was confirmed by plan-view and cross-sectional transmission electron microscopy. © 2000 Elsevier Science B.V. All rights reserved.

Keywords: CdSe/ZnSe; Stranski-Krastanow growth mode; Quantum dots; Excitons

1. Introduction

Quantum dot (QD) structures based on II-VI semiconductors are presently of significant interest due to their advantageous linear and non-linear optical properties as compared to higher-dimensional structures. For the CdSe/ZnSe system two distinguishable classes of QDs were identified: fractional monolayer islands grown by strain-modified island growth (type A) (e.g. Ref. [1]) and three-dimensional (3D) islands grown in Stranski-

Krastanow (SK) mode (type B) (e.g. Ref. [2]). In structures containing type A islands thermal stability and resonant gain were demonstrated in combination with ternary [3] or quaternary [4] II-VI matrix. Although type B islands provide deeper localisation, resonant room-temperature gain could not be demonstrated. This is caused by a too large size of strain-relaxed islands [2] or the appearance of a second island class of a higher density (e.g. Ref. [5]). Probably, the growth of type B islands is often accompanied by the formation of such a second island type. Currently, the simultaneous appearance of different island types in such structures is not considered. In this work, we present methods to distinguish different island types, and we determine the parameters for the growth of structures containing predominantly type B islands.

* Corresponding author. Tel./Fax: + 49-30-314-22054/64.

E-mail address: marburg@physik.tu-berlin.de (M. Straßburg).

¹ On leave from: Ioffe-Institute, Polytechnicheskaya 26, St. Petersburg 194021, Russia.

2. Experimental procedure

The samples were grown by molecular-beam epitaxy (MBE) as described in Ref. [6]. The structures consist of 2.3–3.1 monolayers (ML) CdSe deposited at $T = 260^\circ\text{C}$ sandwiched between two strained pseudomorphic ZnSe layers of 45 nm thickness. All samples were grown on GaAs (001) substrates. The formation of 3D islands was confirmed by in situ monitoring of the RHEED patterns. The structural properties were studied by transmission electron microscopy (TEM) using a Philips CM 200 FEG/ST electron microscope with an electron energy of 200 keV and a Scherzer resolution of 0.24 nm. The Cd distribution was determined by the CELFA evaluation procedure [7]. Optical properties were investigated by cathodoluminescence (CL), photoluminescence (PL), PL excitation (PLE) and gain spectroscopy at temperatures between 1.8 and 300 K. CL measurements were performed using a Jeol JSM 840 scanning electron microscope. The spatial resolution of the CL amounts to 350 nm and the spectral resolution 0.4 meV [8]. PL was excited using a He–Cd laser, the PLE excitation source was the light of a tungsten lamp dispersed by a 0.5 m monochromator. Luminescence was detected by a photomultiplier attached to a 0.85 m double monochromator.

3. Results and discussion

TEM and high-resolution (HR) TEM investigations give evidence for the coexistence of type A and B islands. Fig. 1a shows a plan-view TEM image of a sample with 2.8 ML CdSe deposition confirming the appearance of type B islands. The lateral diameter of these islands is about 16 nm. Additionally, some large islands with a diameter of about 50 nm are observed. Such islands are formed by the coalescence of type B islands. But their large size leads to a plastic strain relaxation resulting in structural defects so that non-radiative recombination dominates.

Type A islands were revealed as a speckle contrast in plan-view TEM and in cross-sectional HRTEM images of the same sample. A typical cross-section HRTEM image of a 2.3 ML sample

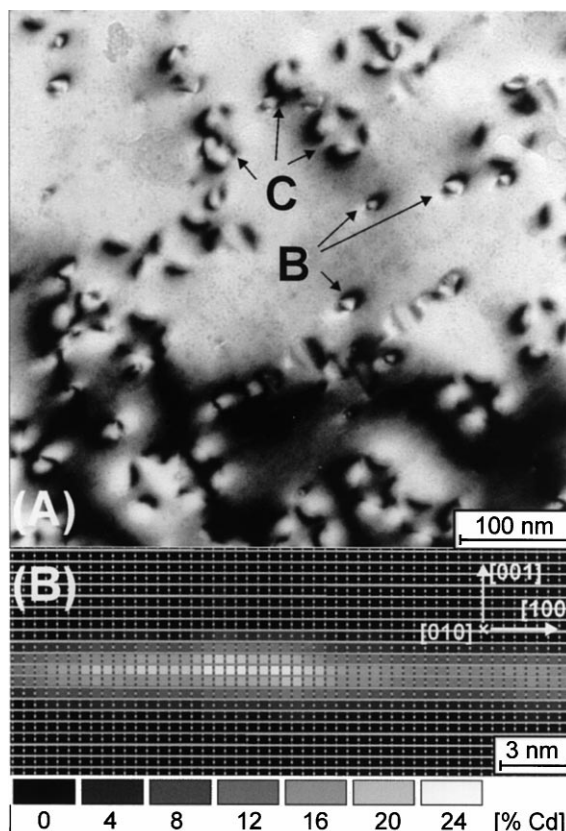


Fig. 1. (a) Plan-view bright field TEM of a CdSe/ZnSe sample with 2.8 ML CdSe. (b) Cross-section image of a sample with 2.3 ML CdSe evaluated by CELFA (taken from Ref. [11]).

evaluated by CELFA is shown in Fig. 1b. The Cd content in the area of the wetting layer is less than 100% and exhibits an inhomogeneous distribution. Obviously, segregation and interdiffusion leads to a broadening of the wetting layer (WL) up to 3 nm in growth direction, and therefore to the formation of a ZnCdSe alloy quantum well. Areas in the WL with increased Cd content (bright areas) represent type A islands which were also found in fractional ML structures (e.g. Ref. [9,10]). These islands have a lateral extension below 10 nm. The Cd content of the type A islands and of the wetting layer exhibited a remarkable dependence on the CdSe coverage as shown in Table 1. A continuous rise of the Cd content with increasing CdSe coverage is determined, whereas the density of type A islands does

not show such dependence. At the same time an increasing CdSe leads to an increase of the density of type B islands.

Table 1

Cd content of wetting layer and type A islands for varied CdSe coverages as determined by CELFA analysis of cross-section high-resolution TEM. The density of the type B islands was obtained by plan-view TEM. The density of type A islands of $5 \times 10^{11} \text{ cm}^{-2}$ shows no dependence on the CdSe coverage

CdSe coverage (ML)	Cd content (%)		Density of type B islands (cm^{-2})
	Wetting layer	Type A islands	
2.3	13	25	1×10^9
2.6	15	30	1×10^{10}
2.8	16	32	2.5×10^{10}
3.1	18	35	5×10^{10}

The zero-dimensional character of excitons localized in the islands was confirmed by spatially (Fig. 2a and b) and spectrally (Fig. 2c and d) resolved CL investigations. Fig. 2a and b show CL images recorded on the low- and high-energy tail of the emission peak, respectively. For detection energies on the low-energy side of the emission peak monochromatic CL images show distinct luminescent areas (Fig. 2a). This observation suggests a low areal density of type B islands which should have a predominantly low emission energy. On the high-energy side of the luminescence peak monochromatic CL images show only a cloudy luminescence distribution (see Fig. 2b). This can be due to a very high areal density of type A islands which predominantly emit in this spectral region. This assumption is supported by CL-spot spectra which on both sides of the luminescence show sharp emission peaks suggesting zero-dimensional recombination processes.

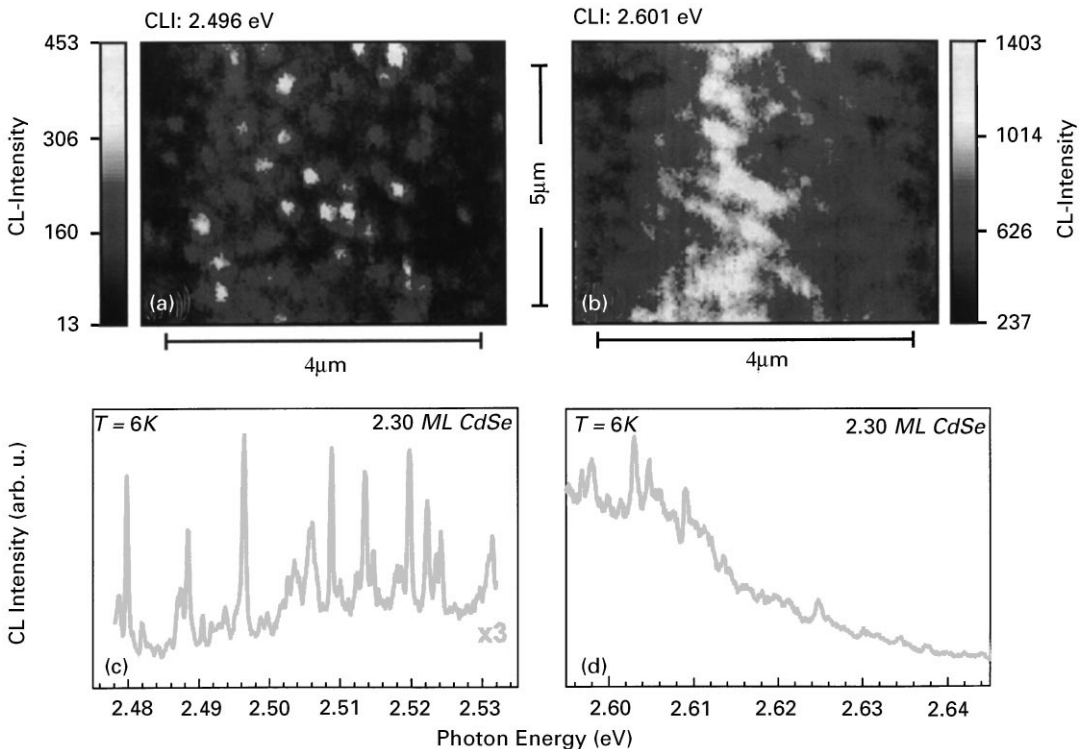


Fig. 2. Monochromatic cathodoluminescence intensity images (a, b) and spot spectra (c, d) of the sample with 2.3 ML CdSe, recorded at $T = 6 \text{ K}$.

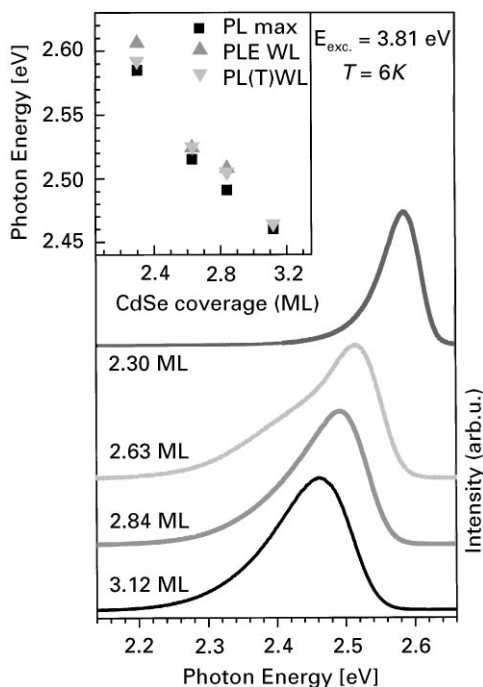


Fig. 3. Photoluminescence (PL) spectra of samples with varied CdSe coverages. Inset: energy positions of the wetting layer (WL), obtained by PLE and temperature-dependent PL, and maximum of the PL emission band as a function of the CdSe coverage.

Fig. 3 shows the emission properties of the quantum islands and the influence of the WL for single layer samples with CdSe coverages varying between 2.3 and 3.1 ML. The broad PL emission bands exhibiting an asymmetric shape were assigned to the radiative recombination of zero-dimensional excitons in type A and B islands. With an increasing CdSe coverage the PL maximum shifts to lower energies and the full-width at half-maximum (FWHM) increases. The structural investigations suggest the increasing density of type B islands with increasing CdSe coverages. This explains the increasing intensity of the low-energy tail of the emission band and the resulting increase of the FWHM. To clarify, the origin of the shift of the PL maximum to lower energies with increasing CdSe coverages we performed PLE and temperature-dependent PL studies. The energy of excitons in the WL, determined by PLE and temperature-

dependent PL (see also Ref. [11]), and the maximum of the PL emission band are displayed in the inset of Fig. 3 as a function of the CdSe coverage. The energy of the WL-state and the PL emission band have the same dependence on the CdSe coverage. With regard to the dependence of the Cd content in the wetting layer and in the type A islands on the CdSe coverage, this behaviour suggests that the PL band is dominated by type A islands. The growth process which is described in Ref. [6] in more detail is therefore believed to induce the formation of type A islands.

4. Conclusion

A clear distinction of CdSe islands in CdSe/ZnSe samples, formed either by strain-modified island growth (type A) or the Stranski–Krastanow mode (type B), is presented based on structural characterisation and optical spectroscopy. Different optical properties are observed due to different localisation energies and pronounced differences in size, shape and Cd content. Embedding between 2.3 and 3.1 ML of CdSe in a pseudomorphically grown ZnSe-matrix leads to the coexistence of both types of islands which both provide a 3D confinement for excitons.

References

- [1] N.N. Ledentsov, I.L. Krestnikov, M.V. Maksimov, S.V. Ivanov, S.V. Sorokin, P.S. Kop'ev, Zh.I. Alferov, D. Bimberg, S.M. Sotomayor Torres, *Appl. Phys. Lett.* 69 (1996) 1343.
- [2] M. Arita, A. Avramescu, K. Uesugi, I. Suemune, T. Numal, H. Machida, N. Shimoyama, *Jpn. J. Appl. Phys.* 36 (1997) 4097.
- [3] R. Engelhardt, U.W. Pohl, D. Bimberg, D. Litvinov, A. Rosenauer, D. Gerthsen, *J. Appl. Phys.* 86, (1999) 5578.
- [4] I.L. Krestnikov, M.V. Maximov, A.V. Sakharov, P.S. Kop'ev, Zh.I. Alferov, N.N. Ledentsov, D. Bimberg, C.M. Sotomayor Torres, *J. Crystal Growth* 184/185 (1998) 545.
- [5] M. Rabe, M. Lowisch, F. Henneberger, *J. Crystal Growth* 184/185 (1998) 248.
- [6] D. Schikora, S. Schwedhelm, D.J. As, K. Lischka, D. Litvinov, A. Rosenauer, D. Gerthsen, M. Strassburg, A. Hoffmann, D. Bimberg, *Appl. Phys. Lett.* 76 (2000) 418.

- [7] A. Rosenauer, U. Fischer, D. Gerthsen, A. Förster, *Ultra-microscopy* 76 (1999) 49.
- [8] J. Christen, U. Roessler (Eds.), *Advances in Solid State Physics*, Vol. XXXIII, Vieweg, Braunschweig, 1990, p. 239.
- [9] M. Strassburg, V. Kutzer, U.W. Pohl, A. Hoffmann, I. Broser, N.N. Ledentsov, D. Bimberg, A. Rosenauer, U. Fischer, D. Gerthsen, I.L. Krestnikov, M.V. Maximov, P.S. Kop'ev, Zh.I. Alferov, *Appl. Phys. Lett.* 72 (1998) 942.
- [10] T. Kümmel, R. Weigand, G. Bacher, A. Forchel, K. Leonardi, D. Hommel, H. Selke, *Appl. Phys. Lett.* 73 (1998) 3105.
- [11] M. Strassburg, Th. Deniozou, A. Hoffmann, R. Heitz, U.W. Pohl, D. Bimberg, D. Litvinov, A. Rosenauer, D. Gerthsen, S. Schwedhelm, K. Lischka, D. Schikora, *Appl. Phys. Lett.* 76 (2000) 685.